

Incorporating Task Progress Knowledge for Subgoal Generation in Robotic Manipulation through Image Edits

Xuhui Kang, Yen-Ling Kuo
University of Virginia
{xuhui, ylkuo}@virginia.edu

Abstract

Understanding the progress of a task allows humans to not only track what has been done but also to better plan for future goals. We demonstrate TaKSIE, a novel framework that incorporates task progress knowledge into visual subgoal generation for robotic manipulation tasks. We jointly train a recurrent network with a latent diffusion model to generate the next visual subgoal based on the robot’s current observation and the input language command. At execution time, the robot leverages a visual progress representation to monitor the task progress and adaptively samples the next visual subgoal from the model to guide the manipulation policy. We train and validate our model in simulated and real-world robotic tasks, achieving state-of-the-art performance on the CALVIN manipulation benchmark. We find that the inclusion of task progress knowledge can improve the robustness of trained policy for different initial robot poses or various movement speeds during demonstrations. The project page is available at <https://live-robotics-ua.github.io/TaKSIE/>.

1. Introduction

Teaching robots to perform complex tasks usually involves turning a task into a sequence of *subgoals*, several steps towards the overall task goal. Several hierarchical methods have been proposed to generate subgoals and have low-level policies to learn to reach the generated subgoals, e.g., task and motion planning [9], options in reinforcement learning [35], and learning hierarchical policies [30, 42].

Effectively generating subgoals requires the robot to understand how a task may progress and the key steps for completing a task. Without this knowledge, the robot may over- or under-generate subgoals. Over-generating subgoals may lead to inefficiency in plan execution because this introduces unnecessary intermediate steps for the robot to achieve. Under-generating subgoals may hurt task performance as each subgoal is still hard for the robot to

achieve. Furthermore, if the robot does not understand the task progress, it may synthesize inconsistent subgoals, especially when the solution distribution is multimodal. For example, for the task “pick up a cup”, if there are multiple cups, the robot may generate the first subgoal to move towards one cup, but have the second subgoal that makes the robot move to another cup at midway. Only when having the task progress knowledge, the robot can generate the subgoals that represent the key steps of a task as in Fig. 1.

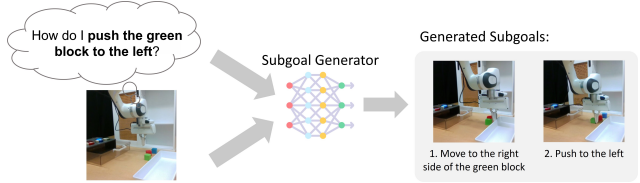


Figure 1. An illustration of the idea that a robot generates the visual subgoals incrementally (shown as the increasing numbers) for an input language command. Note that these images are generated using our subgoal generator. The generated subgoals reveal that the robot needs to understand the precondition, e.g., empty the gripper before grasping, and the preferred pose for grasp, e.g., moving it to the right side of the block.

In this paper, we proposed TaKSIE, a framework that incorporates **T**ask **P**rogress **K**nowledge for **S**ubgoal generation in robotic manipulation through **I**mage **E**ditting, as illustrated in Fig. 2. The subgoals in TaKSIE are represented as images that explicitly tell the robot the physical configurations to achieve. They are used to guide the rollout of the low-level policy. We leverage latent diffusion models to generate visual subgoals as in [17] and [3]. However, most works only consider a fixed interval strategy in subgoal generation, i.e., generating the next subgoals every fixed number of time steps. This strategy usually generates a large number of subgoals if using a small interval or misses the important steps if using a large interval. Tuning the interval to make it work across scenarios is very challenging. In TaKSIE, we use the visual representations pretrained from videos as the implicit task progression knowledge. We imbue this knowledge into language-conditioned robotic ma-

manipulation tasks in two ways. First, it is used to select ground-truth subgoals from demonstrations so we can co-train the subgoal generator and a progress encoder to predict the next visual subgoal based on language commands, the robot’s current state, and ongoing task progression. Second, we add a progress evaluation using this representation to measure whether a generated subgoal is achieved so we can generate subgoals adaptively. We train and test our models on the simulated and the real robot demonstrations showing that our generated subgoals can effectively guide the robot to complete manipulation tasks and achieve state-of-the-art performance on the CALVIN benchmark [24].

This work makes the following contributions:

1. We present a novel framework, TaKSIE, that incorporates task progress knowledge into language-conditioned manipulation tasks.
2. We show how understanding task progress can help generate subgoals that follow the progress of tasks.
3. We demonstrate how the improved visual subgoals can guide low-level policy to improve task performance.

2. Related Work

2.1. Learning Goal-Conditioned Policies

Goal-conditioned policies enable robots to generate actions for a specified goal, either represented in a natural language sentence [22, 23] or an image depicting the desired state [28]. Most approaches use a pretrain text or image encoder to turn language or visual goals into embeddings to condition the policy network to generate actions. While language goals are more expressive, it is harder to acquire annotated demonstration data. On the other hand, visual goals can only represent one specific goal configuration, and we can leverage a large amount of unannotated trajectories to train policy. In TaKSIE, our subgoal generation process effectively turns a language-goal-conditioned problem into a visual-goal-conditioned problem, so it is possible to leverage unannotated trajectories to solve the manipulation tasks specified in natural language.

2.2. Planning with Diffusion Models

Diffusion models have demonstrated the ability to effectively approximate and re-generate data distributions such as in image generation [13, 41] and robotic action generation [1, 5, 15, 40]. Several diffusion-based policy models have been proposed, for example, diffuser [15] refine policies from noise, decision diffuser [1] integrates constraints and skills, and LCD [39] conditions latent plans on language for task execution. Different from these policy models that generate actions, our approach generates visual subgoals with diffusion models to enhance policy guidance. The model closest to us is SuSIE [3] which also leverages the diffusion model for the generation of vi-

sual subgoals. Unlike SuSIE which uses fixed intervals to generate subgoals, we focus on incorporating and tracking task progress in the subgoal generation process. Other than image-based subgoals, other works explore generating short videos to guide the policy [2, 8, 18]. However, generating full video sequences usually requires much more computing resources.

2.3. Task Understanding for Robotic Tasks

To understand what the next subgoals can be, the robot needs to learn the relevant key steps for a task. This knowledge has been encoded as task plans in predefined domains [10, 16]. Another way to represent task progress is using visual keyframes [17, 26]. Recently, large language models (LLMs) have demonstrated the ability to generate task plans or control programs for a variety of robotic tasks [19, 31]. However, LLM-based approaches require converting a state into textual descriptions to synthesize the prompts and assume that a set of API calls exists. To generate visual subgoals that are useful for a visual-goal-conditioned policy, we need to consider task knowledge in the subgoal generation process. Several previous works have explored the use of human videos to help robot learning [29, 32, 37] as they implicitly encode task knowledge. To scale this up, recent works like R3M [25], LIV [20], and VC-1 [21] train on diverse and large-scale human video data to learn useful visual task representations for robotic tasks. Our approach is keyframe-based but leverages these visual representations to measure task progress and enhance the consistency in generation using a progress encoder.

3. Incorporating Task Progress Knowledge for Subgoal Generation through Image Edits

3.1. Problem Formulation

We aim to develop a generative model \mathcal{G} that generates the next key visual subgoal f_{gen} for a task described in natural language, i.e., a language goal. For a sequence of generated images $\{f_{gen}\}$, it needs to be a sequence of subgoals to reach the specified language goal. The generative model is conditioned on the subgoals the robot has reached so far $s_0 \dots s_t$ which indicates the progress and the corresponding language goal l^* . We train this generative model by minimizing the distances between the generated visual subgoals and the corresponding ground-truth subgoals τ_t sampled from the trajectory $\mathcal{T}_{0:T}$ collected from demonstrations:

$$\min_{\theta} \mathbb{E}_{\tau_t \sim \mathcal{T}_{0:T}} [\text{dist}(\mathcal{G}_{\theta}(f_{gen} \mid s_0, \dots, s_t, l^*), \tau_t)] \quad (1)$$

Given a visual subgoal f_{gen} , we aim to have a low-level policy $\pi_{\psi}(a_t \mid s_t, f_{gen})$ that output actions to achieve the subgoal f_{gen} . This policy can be learned from demonstrations.

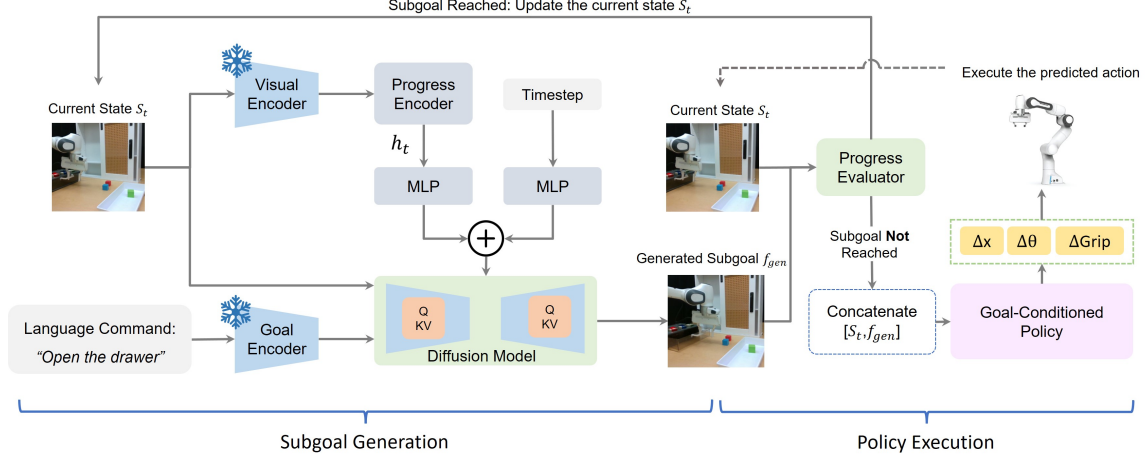


Figure 2. An overview of TaKSIE, a framework that incorporates task progress knowledge (encoded in the Progress Encoder and Progress Evaluation) into language-conditioned robotic manipulation tasks using generated subgoals as its conditions for a low-level policy.

3.2. Framework Overview

Fig. 2 is an overview of the proposed framework which is a two-stage framework: 1) visual subgoal generation and 2) a subgoal-conditioned policy. In the first stage, we generate subgoals based on the image of the initial observation, the natural language sentence about the task, and an embedding of the current task progress from the progress encoder. These generated subgoals serve as intermediate objectives for the robot to achieve. In the second stage, TaKSIE utilizes these generated subgoals to condition the low-level policy. Since we generate visual subgoals autoregressively, we will roll out the low-level policy until it reaches the current subgoal and use this updated state to generate the next subgoal. Ideally, the low-level policy π_ψ should predict the termination. However, as the generated visual subgoals may not perfectly match the ground-truth subgoals, it is hard to learn the termination for the generated subgoal. We employ a progress evaluator to determine if the generated subgoal is reached or the low-level policy does not make progress so we need to generate the next visual subgoal for policy rollout. Once the progress evaluator decides to advance to the next subgoal, the input of the subgoal generator is replaced with the updated state s_{t+i} . This update initiates a new round of subgoal generation, allowing the robot to proceed with a new round of subgoal execution.

3.3. Incorporating Task Progress

To consider task progress in subgoal generation, we need to first have a measure of whether a state is making progress toward completing a task. Then we can use this measure to 1) identify the key states for a task and train the subgoal generation using the identified key states and 2) evaluate whether a subgoal is reached. Recent visual representations pretrained using time contrastive learning on ego-centric videos, such as R3M [25] and LIV [20], implicitly encode

the task progress knowledge. They are usually trained by minimizing the distance between temporally close frames while maximizing distant or unrelated ones, which can capture the essential features for sequential task progression. In TaKSIE, we utilize this pretrained visual representation \mathcal{M} to measure the task progress.

3.3.1 Ground-truth Subgoal Selection

Given a demonstration of a manipulation task $\{s_0, \dots, s_T\}$, we use the following strategy to select the ground-truth subgoals. First, for each state s_i in the demonstration, we calculate the distance between this state and the final goal state s_T using the L2 norm of the time-contrastive visual representation: $\|\mathcal{M}(s_i) - \mathcal{M}(s_T)\|_2$. Second, after getting the distance curve of each frame, we will smooth the curve by LOWESS [6]. Third, we can calculate the slope I_i of each frame and normalized them into the range $[0,1]$. Finally select s_i as ground truth subgoal by $I_{i-1} > \delta_1$ and $I_{i+1} < \delta_2$ where δ_1 and δ_2 are two hyper-parameters to control the slope change. We also set a minimum subgoal interval d to avoid selecting adjacent frames.

This definition means that these are the points we need to reach first, then to make obvious progress. Fig. 3 shows an example of measured task progress using this distance. The two selected subgoals for the task “open the drawer” are shown in the right of Fig. 3 indicating that the robot needs to first move above the drawer handle and then insert its gripper into the handle.

But if we use a fixed-interval selection strategy as in [3], this selects a variety of subgoals depending on how fast human demonstrators move and the interval size we choose. In the example of opening the drawer, an interval like 16 time steps will select only two subgoals, the first moving towards the handle, and the second inserting the gripper into the handle, but moving from the first subgoal to the second is still

hard for the robot as it still needs to find the alignment for inserting the gripper.

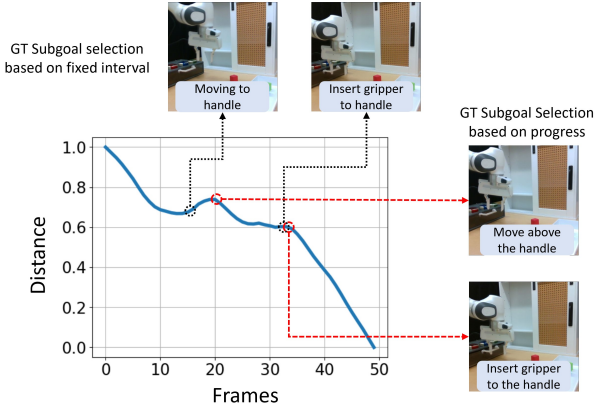


Figure 3. Comparison between TaKSIE ground-truth (GT) subgoal selection (red arrows, two frames on the right) and fixed-interval subgoal selection (black arrows, two frames at the top).

3.3.2 Progress Encoder

Selecting the key steps as the ground-truth subgoals for training the subgoal generator only helps instruct the robot to generate subgoals that are close to key steps. However, many tasks can be solved in different ways, i.e., multimodal solutions. For example, to slide the door to the right, the robot can choose to grab the handle to move the door to the right or put its gripper to the left of the handle to push it to the right. The generation of two consecutive subgoals may still be inconsistent so the robot will switch between modes and fail to finish the task. To enforce consistency in subgoal generation, we create an external memory, a progress encoder, to keep track of the subgoals achieved so far and guide the next subgoal. The progress encoder is a recurrent network that takes the image of the current state s_t and the last hidden state h_{t-1} of the progress encoder to update its hidden state. The output hidden state h_t is the progress embedding that is used in the subgoal generator.

3.3.3 Progress Evaluator

Since our generated subgoals are not in a fixed interval, we need to determine when to generate the next subgoal instead of generating in fixed time steps. The progress evaluator assesses the updated current state by comparing its representation with the generated visual subgoal. If the subgoal is nearly achieved or remains unachieved after a significant amount of time, the updated state is then fed into a new round of subgoal generation.

Again, we use the pretrained time-contrastive visual representations to measure if the current state and the generated subgoal are in similar progress. We use cosine similarity as the similarity measurement. If the similarity reaches δ or

the step for the current subgoal is larger than λ , it will move forward to the next subgoal. This process ensures continuous progress toward the achievement of the overall goal.

3.4. Models

3.4.1 Subgoal Generator

The subgoal generator is a conditional generative model. We implement this generator using a 2D image-conditioned diffusion model, allowing flexibility in the choice of the model, e.g., ControlNet [41] or InstructPix2Pix [4]. A detailed analysis of these choices can be found in Appx. D. The diffusion model conditions on image observations to ensure the generation follows the conditions:

- The current state s_t . This condition informs the generator to keep the existing objects and the environment.
- The natural language description of goal state l^* . This condition shows how an object should be manipulated.
- The progress embedding h_t . This condition adds time-relevant constraints and provides task-specific information to enable the generator to interpolate between the current and the goal state.

The image of the current state s_t is used as input to the conditioned generative model to ensure the generated subgoal image includes objects in the current state.

The language goal is encoded by a pretrained text encoder, e.g., the CLIP text encoder. This embedding of the goal is fused with the progress embedding h_t and the diffusion time step to condition on each level of the U-Net. Conditioning on goal and progress on each level allows us to generate images that match the next subgoal.

During the diffusion process, we use classifier-free guidance [14] to improve the quality of the generated images. It includes text guidance to encourage the generation far from the negative prompt, usually a blank string, and image guidance to encourage the generation close to the current image. Specifically, we use the antonyms of words to generate the negative prompts, e.g., “close the drawer” is the negative prompt for “open the drawer”. The guidance ensures the generated image is in the correct task and keeps objects unrelated to the goal unchanged.

3.4.2 Subgoal Conditioned Policy

We use a policy network parameterized by ϕ to predict actions that achieve the generated subgoals. This policy network $\pi_\phi(a|s_t, f_{gen})$ takes the current state s_t and the generated subgoal f_{gen} to decode into the 6-DoF pose changes for the robot’s end-effector and the gripper action (i.e., open or close). We learn this policy from human demonstrations.

3.5. Training Pipeline

We train the subgoal generator and the policy separately.

Training the Subgoal Generator We first fine-tune the diffusion model with the selected ground-truth subgoal images. This fine-tuning process allows us to generate images that match the style of the environment. We then initialize the conditioned generative model with weights from the fine-tuned diffusion model. For ControlNet, we copy the weights to the branch and co-train with the U-Net branch. For InstructPix2Pix, we apply the weights to the full model and train. This co-training process enables us to jointly learn to track the task progress and accurately predict the next visual subgoal in the sequence. To ensure the successful prediction of the next subgoal, we adopt the MSE loss, \mathcal{L}_{gen} , to compare the generated subgoal, f_{gen} and the ground-truth subgoal, f_{gt} :

$$\mathcal{L}_{gen}(f_{gen}, f_{gt}) = \sum (f_{gen} - f_{gt})^2 \quad (2)$$

Training the Goal-conditioned Policy We train the policy network with goal-conditioned behavior cloning (GCBC). To increase the variety of the initial state and the goal state observed by the goal-conditioned policy, we randomly sample subtrajectories from the human demonstration dataset \mathcal{D} using window sizes ranging from k_{min} to k_{max} . To better reach the final goal, we repeat the final state k_δ times. In our implementation, we use a diffusion policy based GCBC (D-GCBC) and thus use a similar loss function as Eq. (2) but we replace image f with action a .

4. Experiments

4.1. Dataset and Evaluation Environment

We evaluated TaKSIE in both simulated and real-world robotic environments. Each environment consists of a Franka Emika Panda robot arm performing tabletop manipulation with a drawer, cabinet slider, and some colored blocks as well as light switches.

Simulation We train and test our models using the CALVIN benchmark [24], a benchmark for long-horizon language-conditioned manipulation tasks. Similar to prior works [22, 23, 39], we use Task D for evaluation, which consists of 34 different tabletop manipulation tasks. The training set contains more than 5,000 trajectories with an average length of around 64. The evaluation for Long-Horizon Multi-Task Language Control (LH-MLTC) in CALVIN involves 1,000 task sequences, each containing five tasks. We use LH-MLTC to show how incorporating task progress can improve tasks at different horizons.

Real-world To show our proposed framework can be integrated with the real robot, Franka Research 3. We designed 28 tasks that resemble the tasks in CALVIN. For example, opening the drawer, turning on the red LED, placing

the red block in the box, etc. For each task, we used an Oculus VR controller to teleoperate the robot to collect 50 trajectories to use as our training set. We record the trajectories at 30Hz but downsample to 15Hz for training. Each trajectory includes a language command for the task, a sequence of still images from an over-the-shoulder camera, and a sequence of end-effector pose and gripper state corresponding to the image observation. Unlike the trajectories in CAVLIN which are of similar length, the real-world trajectories have various trajectory lengths ranging from 10 to 104. At the evaluation phase, we randomized our environment configuration and tested each task 5 times.

4.2. Experiment Setup

4.2.1 Baselines

We compare TaKSIE with the following methods which have strong performance in language-conditioned robotic manipulation tasks like CALVIN.

- **HULC** [23]: HULC is a hierarchical, language-conditioned imitation learning method.
- **LCD** [39]: LCD combines language with diffusion models for hierarchical planning in a latent plan space.
- **D-LCBC** [36]: D-LCBC enhances the language-conditioned behavior cloning (LCBC) [34] framework by incorporating a diffusion process with the DDIM objective. Following [36], we employed a ResNet-50 [12] to encode observations and MUSE sentence embedding [38] to encode language commands.
- **SuSIE** [3]: Similar to TaKSIE, SuSIE employs diffusion models to generate subgoals that guide the low-level policy, but it was trained and evaluated at fixed intervals. We retrain SuSIE using the implementation and configuration provided in the original repository.

In the CALVIN evaluation, we compare TaKSIE with existing methods, including HULC, LCD, and SuSIE. It is important to note that the top-performing models on CALVIN use additional information in their policy networks. For example, HULC and LCD use extra gripper images in their observations. HULC++ [22] uses an LLM to decompose language annotations and depth images as reconstruction targets during training. In contrast, TaKSIE only uses a static RGB image as observation. In our real-world evaluation, we trained SuSIE and D-LCBC [36] for comparison.

4.2.2 Implementation Details

We consider three pre-trained visual encoders:

1. **CLIP** is a widely used representation trained with contrastive learning using language annotation for objects.
2. **R3M** is an unimodal representation trained with time-contrastive learning so it implicitly encodes progress knowledge of tasks.

3. **LIV** is a multi-model representation trained with time-contrastive learning on videos with language annotations so it does not only encode the progress knowledge but is also aware of the task semantics.

We select one of these three visual representations for subgoal selection and the input of the GRU progress encoder. The progress evaluator was a fine-tuned LIV model with 10k steps to make it work better in our environment.

Ground-truth (GT) Subgoals Selection We use the selected visual representation to calculate the distance of each frame to the final frame. Then we smooth the distance curve using a smooth factor 0.167, and set $\delta_1 = 0$, $\delta_2 = 0$, and minimum subgoal interval $d = 7$ to avoid the impact of outliers. On average, in CALVIN, we select 2.74 ground-truth subgoals, including the final goal, with an interval of 16.4; in the real robot experiment, we select 1.6 ground-truth subgoals with an interval of 23.

Training Generative Model In all experiments, we use the pretrained weights from [27] to initialize our diffusion model. However, training a high-quality generative model requires a fair amount of images. Instead of only training with subgoal images, we first fine-tune the unconditional diffusion model using all frames in the recorded trajectories. On average, there are 64 images per trajectory in CALVIN and 32 images per trajectory for the real robot dataset. The unconditioned diffusion model is trained for 100k steps with batch size 256. This is a key step to generate realistic images. After this, we can effectively use the subgoal images to train the conditional model to follow progress. The original ControlNet freezes the U-Net branch and trains only the ControlNet branch. We found that training the diffusion model together with the ControlNet branch yielded a better image quality than keeping the diffusion model part frozen. We use the weights of the trained unconditional diffusion model to initialize the ControlNet part. Finally, we trained InstructPix2Pix or ControlNet with batch size 256 for 300k training steps. This training procedure allows us to effectively use the limited amount of demonstration data to generate high-quality subgoal images.

Goal-Conditioned Policy We use a diffusion model based goal-conditioned policy (D-GCBC) [36] as our policy network. We stack the current observation and the goal image, encode them with ResNet-50, and then use this embedding to condition a 3 256-unit layers MLP model. Following [3, 5], we predict four action sequences for temporal consistency and do a dimension-wise mean of them. In CALVIN, we set $k_{min} = 8$ and $k_{max} = 20$ as our minimum and maximum ground-truth subgoal interval is 8 and 32. In real-world experiments, we set $k_{min} = 4$ and $k_{max} = 20$. Both models are trained in 400k steps with batch size 256.

Goal Image Type	Avg. Success Rate
Ground-truth final goal only	50.57%
Ground-truth Subgoals	86.15%
TaKSIE (Ours, w/ R3M)	86.84%

Table 1. Success rate on CALVIN validation set across types of goal images. Our results show that subgoal images significantly improve the task performance and our generated subgoals can achieve a similar rate as the ground-truth subgoals.

4.2.3 Policy Rollout

At inference, our subgoal generator uses DDIM [33] with 50 time steps and with text and image classifier-free guidance scales set to 2.5. Our progress evaluator sets the cosine similarity threshold δ to 0.96. The maximum number of rollout steps λ for a subgoal image is 20.

4.3. Results

4.3.1 Quality of Generated Subgoals

To assess the quality of the generated subgoals, we compare our task success rate against the policy conditioned on the ground-truth (GT) goal images. The condition that only uses the GT final goal shows the performance of good image quality of the goal but does not consider the task progress so only one goal is used. The condition that uses the GT subgoal images uses our progress evaluation to determine whether to move to the next subgoal. This represents the performance of subgoals when the subgoals have good image quality and a good understanding of task progress. During rollouts, we use the same policy network and parameters for these conditions. We run this evaluation on the CALVIN validation set which has 34 tasks, and around 30 rollouts per task. Tab. 1 showed that the subgoals generated by TaKSIE can lead to a similar success rate as using GT subgoals, indicating that our generated subgoals are as good as the ones selected from the human demonstrations.

4.3.2 Results on Simulation

Fig. 4 shows an example rollout of TaKSIE in CALVIN for the task “rotate the blue block to the left.” The first generated subgoal correctly instructs the robot to grab the blue block. Then in the second generated subgoal, rotate the blue block a bit to the left. Finally, the last subgoal shows the configuration when the task is successful.

Tab. 2 compares the success rates of TaKSIE and SOTA methods in the CALVIN LH-MTLC setting across different horizons. TaKSIE can achieve a higher success rate for all horizons Especially, the improvement gets more significant when the number of instructions increases. We find that unlike the first task which always starts from a natural pose, the 2nd to 5th tasks start from the end pose of the previous task. This makes it hard for the fixed interval strategy such as SuSIE to generate the subgoals that are useful to the

Method	Input RGB Type	CALVIN Train D \rightarrow Test D, LH-MTLC						
		No. Instructions in a Row (1000 chains)						
		1	2	3	4	5	Avg. Len.	
HULC [23]	Static + Gripper	82.7 (0.3)	64.9(1.7)	50.4 (1.5)	38.5 (1.9)	28.3 (1.8)	2.64 (0.05)	
LCD [39]	Static + Gripper	88.7 (1.5)	69.9 (2.8)	54.5 (5.0)	42.7 (5.2)	32.2 (5.2)	2.88 (0.19)	
SuSIE [3]	Static	87.7 (1.3)	67.4 (1.6)	49.8 (3.2)	41.9 (2.3)	33.7 (1.8)	2.80 (0.15)	
TaKSIE (Ours, w/ R3M)	Static	90.4 (0.2)	73.9 (1.0)	61.7 (0.5)	51.2 (0.2)	40.8 (0.6)	3.18 (0.02)	
w/o Progress Evaluator	Static	87.6 (0.3)	72.1 (1.3)	58.8 (1.2)	47.5 (0.1)	38.2 (0.1)	3.04 (0.02)	
w/o Progress Encoder	Static	87.6 (0.2)	72.9 (0.1)	61.0 (0.1)	49.0 (0.8)	40.1 (0.8)	3.11 (0.02)	
w/o Negative Prompt	Static	87.9 (0.4)	72.8 (0.8)	59.5 (1.5)	48.3 (1.6)	38.1 (1.3)	3.07 (0.05)	
TaKSIE w/ LIV	Static	85.7 (1.2)	68.1 (0.8)	52.3 (0.9)	41.7 (0.5)	31.3 (0.8)	2.78 (0.02)	
TaKSIE w/ CLIP	Static	83.9 (0.3)	65.3 (0.5)	49.7 (1.5)	37.7 (1.3)	28.5 (2.2)	2.65 (0.04)	

Table 2. Success rate (%) of TaKSIE on the CALVIN benchmark across 3 runs compared with SOTA (top three rows) and ablations. Our method, using only static images, outperforms baselines that use both static and gripper images, demonstrating the effectiveness of incorporating task progress and subgoal generation in improving task performance.

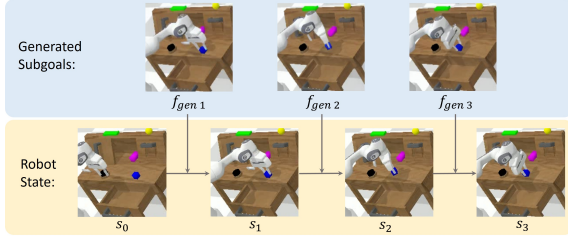


Figure 4. An example rollout demonstrating how the generated subgoals guide the robot for a task: rotate the blue block left.

policy as the key states will be at the various positions of a trajectory. Only ours can generate useful subgoals when the initial pose of a task changes.

4.3.3 Results on the Real Robot

Tab. 3 shows the comparison with D-LCBC and SuSIE in the real-world environment. We grouped similar tasks into the same rows. With only 50 trajectories per task, TaKSIE can reach 93.3% for simple tasks like placing a block in the box and 80.0% for more complex tasks like lifting a block. D-LCBC struggles with most tasks. SuSIE can do well in simple tasks but has much worse performance in more challenging tasks such as moving the slider and lift blocks. We find that our demonstration is collected at different teleoperation speeds and has various lengths, the fix-length subgoal selection and generation strategy does not work well in real-world human demonstrations.

Tasks	SuSIE	D-LCBC	TaKSIE (Ours)
Move slider left/right	30.0	0.0	70.0
Open/close drawer	50.0	20.0	70.0
Turn on R/G/B LED	66.7	13.3	73.3
Turn off R/G/B LED	66.7	6.7	60.0
Place R/G/B block box	86.7	46.7	93.3
Place R/G/B block table	86.7	46.7	80.0
Push R/G/B block left	33.3	13.3	40.0
Push R/G/B block right	66.7	20.0	80.0
Lift R/G/B block from table	20.0	0.0	80.0
Average	56.3	18.5	71.9

Table 3. Success rate (%) for the real-world robotic tasks. TaKSIE outperforms the baselines that do not consider task progress.

4.3.4 Ablations: Framework Components

The middle three rows in Tab. 2 show the impact of different components. We show that removing the progress evaluator (i.e., using a fixed interval) or the progress encoder makes the performance worse. Negative prompts also affect the success rate. Without negative prompts, tasks like pushing or rotating blocks to the left or right may sometimes generate subgoals that move in opposite directions.

4.3.5 Ablations: Visual Representations

The bottom two rows in Tab. 2 show the results of different visual representations. R3M performs best. Compared to CLIP, R3M encodes progress better as it is trained with time-contrastive learning which distinguishes frames more effectively. Compared with LIV which is pretrained on the EPIC-KITCHENS [7], R3M is trained on Ego4D [11] which is a much larger ego-centric video dataset so it shows better generalization to out of domain videos.

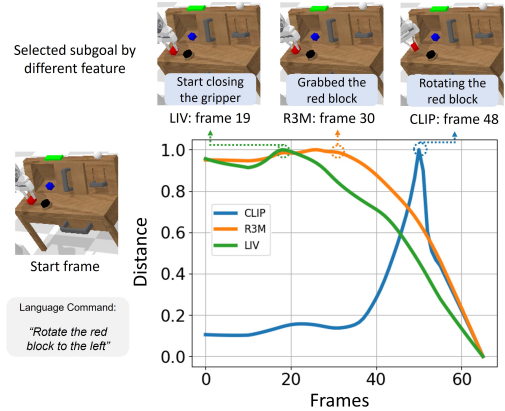


Figure 5. An example for the task “rotate the red block to the left,” illustrating how different embeddings affect subgoal selection.

Fig. 5 shows an example of how different features affect subgoal selection for a task such as rotating a block. LIV selects the frame where the gripper begins to close, which does not provide enough guidance. R3M selects the frame where the block is just grasped, which matches our expected

subgoal. CLIP, however, selects the frame where the block is already rotated, which is almost the same as the final goal. We note that the distance curve sometimes increases, especially for CLIP as it is not trained with time-contrastive learning. While the distance curves in LIV and R3M track progress better, there are still small fluctuations, suggesting future improvements for time-contrastive learning methods.

4.4. Impact of Dataset Size

Our real robot experiments show that we can use fewer demonstrations (1.4k trajectories recorded over 7 hours) than prior works, e.g. 60k trajectories used in SuSIE, to generate subgoal images. To understand the impact of training set size, we further train the models with various dataset sizes on CALVIN. We sampled 75%, 50%, and 25% of the data (i.e., an average of 97, 65, and 33 trajectories for each task) to train all methods to assess how performance changes with reduced data. Tab. 4 shows that even with 25% of data, our success rate remains relatively high. The example subgoal generations can be found in Appx. A.

% of Training Data	100%	75%	50%	25%
TaKSIE (Ours)	86.84	79.96	76.36	73.95
SuSIE	79.73	73.03	70.13	65.13
D-LCBC	70.23	62.14	54.53	50.67

Table 4. Success rates (%) on the CALVIN dataset with different amounts of training data. TaKSIE has a relatively good success rate even when trained on only 25% of the available data.

4.5. Generalization to Unseen Scenarios

To understand the generalization ability of our method, we evaluated task execution in two unseen scenarios.

Unseen Tasks: We select one task from each category (9 tasks in total) in CALVIN as the training set. Then we tested in the same environment but different tasks from the same categories, e.g., test on “push the pink block to the right” but trained on “push the blue block to the left”.

Unseen Environment: We utilized all 34 tasks as in unseen tasks to train TaKSIE in three CALVIN environments (A, B, C) and tested the model on the same tasks but in an unseen env. D (see Appx. B for example environments and generations). Tab. 5 shows that the success rate drops in both cases but ours still outperforms baselines.

4.6. Qualitative Examples

Fig. 6 shows a qualitative comparison between TaKSIE and SuSIE for a task “open the drawer”. Our generated subgoal first guides the robot to insert its gripper into the handle and then moves outwards to open the drawer. In

	Unseen Tasks	Unseen Environment
TaKSIE (Ours)	54.31	73.74
SuSIE	49.64	71.24
D-LCBC	0.04	0.12

Table 5. Success rate (%) of TaKSIE on unseen scenarios.

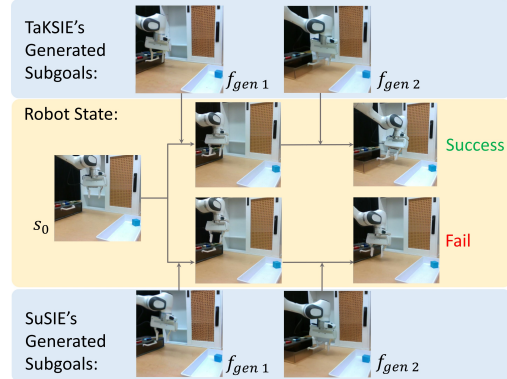


Figure 6. Rollouts comparison between ours and SuSIE’s.

SuSIE’s generation, it generated the subgoals but missed the key state to insert the gripper into the drawer handle, and therefore, failed to complete the task.

4.7. Failure Cases

We observe three types of failure cases (see examples in Appx. C). First, the model may generate incorrect subgoals, for example, it generates pushing a block to the right in the task of pushing it to the left. This indicates that language embedding does not provide sufficient spatial information. Using a more powerful language encoder can help in the future. Second, the model may generate low-quality images, e.g., blurry or distorted regions. Having bad image quality affects the performance of the goal-conditioned policy as it cannot identify the correct visual goals. In TaKSIE, we regenerate subgoal images when the robot does not achieve the subgoal in λ time steps which mitigates the impact of the low-quality images. Third, the policy may fail to reach the subgoal when the generated subgoal is good. This indicates that improvement in the policy is needed.

5. Conclusion & Future Work

We have demonstrated that it is possible to incorporate task progress to generate better visual subgoals to guide the rollout of policies. Instead of using a fixed interval, we showed that the task progress implicitly encoded in the time-contrastive visual representations can help select ground-truth subgoals. Together with a progress encoder and evaluator, TaKSIE can boost the performance of robotic manipulation tasks in simulation and the real world. While our design separates subgoal generation and policy execution into two stages, we may consider cotrain them so both models can be aware of each other’s capability to align representations better. Our current task is fully observable and mostly atomic and sequential. Future work can extend to mobile manipulation and complex task structures. In these scenarios, handling partial observation, changing viewpoints, and dependency of subgoals will be important.

6. Acknowledgment

The authors acknowledge Research Computing at the University of Virginia for providing the computational resources and technical support that made the results in this work possible.

References

- [1] Anurag Ajay, Yilun Du, Abhi Gupta, Joshua Tenenbaum, Tommi Jaakkola, and Pulkit Agrawal. Is conditional generative modeling all you need for decision-making? arXiv preprint arXiv:2211.15657, 2022. 2
- [2] Anurag Ajay, Seungwook Han, Yilun Du, Shuang Li, Abhi Gupta, Tommi Jaakkola, Josh Tenenbaum, Leslie Kaelbling, Akash Srivastava, and Pulkit Agrawal. Compositional foundation models for hierarchical planning, 2023. 2
- [3] Kevin Black, Mitsuhiro Nakamoto, Pranav Atreya, Homer Rich Walke, Chelsea Finn, Aviral Kumar, and Sergey Levine. Zero-shot robotic manipulation with pre-trained image-editing diffusion models. In The Twelfth International Conference on Learning Representations, 2024. 1, 2, 3, 5, 6, 7
- [4] Tim Brooks, Aleksander Holynski, and Alexei A Efros. Instructpix2pix: Learning to follow image editing instructions. In Proceedings of the IEEE/CVF Conference on Computer Vision and Pattern Recognition, pages 18392–18402, 2023. 4
- [5] Cheng Chi, Siyuan Feng, Yilun Du, Zhenjia Xu, Eric Cousineau, Benjamin Burchfiel, and Shuran Song. Diffusion policy: Visuomotor policy learning via action diffusion, 2023. 2, 6
- [6] William S Cleveland. Robust locally weighted regression and smoothing scatterplots. Journal of the American statistical association, 74(368), 1979. 3
- [7] Dima Damen, Hazel Doughty, Giovanni Maria Farinella, Sanja Fidler, Antonino Furnari, Evangelos Kazakos, Davide Moltisanti, Jonathan Munro, Toby Perrett, Will Price, and Michael Wray. Scaling egocentric vision: The epic-kitchens dataset, 2018. 7
- [8] Yilun Du, Mengjiao Yang, Bo Dai, Hanjun Dai, Ofir Nachum, Joshua B. Tenenbaum, Dale Schuurmans, and Pieter Abbeel. Learning universal policies via text-guided video generation, 2023. 2
- [9] Caelan Reed Garrett, Rohan Chitnis, Rachel Holladay, Beomjoon Kim, Tom Silver, Leslie Pack Kaelbling, and Tomás Lozano-Pérez. Integrated task and motion planning. Annual review of control, robotics, and autonomous systems, 4:265–293, 2021. 1
- [10] Caelan Reed Garrett, Tomás Lozano-Pérez, and Leslie Pack Kaelbling. Pddlstream: Integrating symbolic planners and blackbox samplers via optimistic adaptive planning. In Proceedings of the International Conference on Automated Planning and Scheduling, volume 30, pages 440–448, 2020. 2
- [11] Kristen Grauman, Andrew Westbury, Eugene Byrne, Zachary Chavis, Antonino Furnari, Rohit Girdhar, Jackson Hamburger, Hao Jiang, Miao Liu, Xingyu Liu, Miguel Martin, Tushar Nagarajan, Ilija Radosavovic, Santhosh Kumar Ramakrishnan, Fiona Ryan, Jayant Sharma, Michael Wray, Mengmeng Xu, Eric Zhongcong Xu, Chen Zhao, Siddhant Bansal, Dhruv Batra, Vincent Cartillier, Sean Crane, Tien Do, Morrie Doulaty, Akshay Erapalli, Christoph Feichtenhofer, Adriano Fragomeni, Qichen Fu, Abrahm Gebrese-lasie, Cristina Gonzalez, James Hillis, Xuhua Huang, Yifei Huang, Wenqi Jia, Weslie Khoo, Jachym Kolar, Satwik Kot-tur, Anurag Kumar, Federico Landini, Chao Li, Yanghao Li, Zhenqiang Li, Karttikeya Mangalam, Raghava Modhugu, Jonathan Munro, Tullie Murrell, Takumi Nishiyasu, Will Price, Paola Ruiz Puentes, Merey Ramazanova, Leda Sari, Kiran Somasundaram, Audrey Southerland, Yusuke Sugano, Ruijie Tao, Minh Vo, Yuchen Wang, Xindi Wu, Takuma Yagi, Ziwei Zhao, Yunyi Zhu, Pablo Arbelaiz, David Cran-dall, Dima Damen, Giovanni Maria Farinella, Christian Fue-gen, Bernard Ghanem, Vamsi Krishna Ithapu, C. V. Jawahar, Hanbyul Joo, Kris Kitani, Haizhou Li, Richard Newcombe, Aude Oliva, Hyun Soo Park, James M. Rehg, Yoichi Sato, Jianbo Shi, Mike Zheng Shou, Antonio Torralba, Lorenzo Torresani, Mingfei Yan, and Jitendra Malik. Ego4d: Around the world in 3,000 hours of egocentric video, 2022. 7
- [12] Kaiming He, Xiangyu Zhang, Shaoqing Ren, and Jian Sun. Deep residual learning for image recognition, 2015. 5
- [13] Jonathan Ho, Ajay Jain, and Pieter Abbeel. Denoising dif-fusion probabilistic models. In Proceedings of the 34th International Conference on Neural Information Processing Systems, pages 6840–6851, 2020. 2
- [14] Jonathan Ho and Tim Salimans. Classifier-free diffusion guidance, 2022. 4
- [15] Michael Janner, Yilun Du, Joshua Tenenbaum, and Sergey Levine. Planning with diffusion for flexible behavior synthe-sis. In International Conference on Machine Learning, pages 9902–9915. PMLR, 2022. 2
- [16] Yu-qian Jiang, Shi-qi Zhang, Piyush Khandelwal, and Pe-ter Stone. Task planning in robotics: an empirical compari-son of pddl-and asp-based systems. Frontiers of Information Technology & Electronic Engineering, 20:363–373, 2019. 2
- [17] Xuhui Kang, Wenqian Ye, and Yen-Ling Kuo. Imag-ined subgoals for hierarchical goal-conditioned policies. In CoRL 2023 Workshop on Learning Effective Abstractions for Planning (LEAP), 2023. 1, 2
- [18] Po-Chen Ko, Jiayuan Mao, Yilun Du, Shao-Hua Sun, and Joshua B. Tenenbaum. Learning to act from actionless videos through dense correspondences, 2023. 2
- [19] Jacky Liang, Wenlong Huang, Fei Xia, Peng Xu, Karol Hausman, Brian Ichter, Pete Florence, and Andy Zeng. Code as policies: Language model programs for embodied con-trol. In 2023 IEEE International Conference on Robotics and Automation (ICRA), pages 9493–9500. IEEE, 2023. 2
- [20] Yecheng Jason Ma, William Liang, Vaidehi Som, Vikash Kumar, Amy Zhang, Osbert Bastani, and Dinesh Jayara-man. Liv: Language-image representations and rewards for robotic control. arXiv preprint arXiv:2306.00958, 2023. 2, 3
- [21] Arjun Majumdar, Karmesh Yadav, Sergio Arnaud, Yecheng Jason Ma, Claire Chen, Sneha Silwal, Aryan

- Jain, Vincent-Pierre Berges, Pieter Abbeel, Jitendra Malik, et al. Where are we in the search for an artificial visual cortex for embodied intelligence? [arXiv preprint arXiv:2303.18240](#), 2023. 2
- [22] Oier Mees, Jessica Borja-Diaz, and Wolfram Burgard. Grounding language with visual affordances over unstructured data. In *Proceedings of the IEEE International Conference on Robotics and Automation (ICRA)*, London, UK, 2023. 2, 5
- [23] Oier Mees, Lukas Hermann, and Wolfram Burgard. What matters in language conditioned robotic imitation learning over unstructured data. *IEEE Robotics and Automation Letters (RA-L)*, 7(4):11205–11212, 2022. 2, 5, 7
- [24] Oier Mees, Lukas Hermann, Erick Rosete-Beas, and Wolfram Burgard. Calvin: A benchmark for language-conditioned policy learning for long-horizon robot manipulation tasks. *IEEE Robotics and Automation Letters*, 7(3):7327–7334, 2022. 2, 5
- [25] Suraj Nair, Aravind Rajeswaran, Vikash Kumar, Chelsea Finn, and Abhinav Gupta. R3m: A universal visual representation for robot manipulation. In *Conference on Robot Learning*, pages 892–909. PMLR, 2023. 2, 3
- [26] Karl Pertsch, Oleh Rybkin, Jingyun Yang, Shenghao Zhou, Konstantinos Derpanis, Kostas Daniilidis, Joseph Lim, and Andrew Jaegle. Keyframing the future: Keyframe discovery for visual prediction and planning. In *Learning for Dynamics and Control*, pages 969–979. PMLR, 2020. 2
- [27] Robin Rombach, Andreas Blattmann, Dominik Lorenz, Patrick Esser, and Björn Ommer. High-resolution image synthesis with latent diffusion models. *CoRR*, abs/2112.10752, 2021. 6
- [28] Erick Rosete-Beas, Oier Mees, Gabriel Kalweit, Joschka Boedecker, and Wolfram Burgard. Latent plans for task agnostic offline reinforcement learning. In *Proceedings of the 6th Conference on Robot Learning (CoRL)*, 2022. 2
- [29] Karl Schmeckpeper, Oleh Rybkin, Kostas Daniilidis, Sergey Levine, and Chelsea Finn. Reinforcement learning with videos: Combining offline observations with interaction. [arXiv preprint arXiv:2011.06507](#), 2020. 2
- [30] Wonchul Shin and Yusung Kim. Guide to control: offline hierarchical reinforcement learning using subgoal generation for long-horizon and sparse-reward tasks. In *Proceedings of the Thirty-Second International Joint Conference on Artificial Intelligence*, pages 4217–4225, 2023. 1
- [31] Ishika Singh, Valts Blukis, Arsalan Mousavian, Ankit Goyal, Danfei Xu, Jonathan Tremblay, Dieter Fox, Jesse Thomason, and Animesh Garg. Progprompt: Generating situated robot task plans using large language models. In *2023 IEEE International Conference on Robotics and Automation (ICRA)*, pages 11523–11530. IEEE, 2023. 2
- [32] Laura Smith, Nikita Dhawan, Marvin Zhang, Pieter Abbeel, and Sergey Levine. Avid: Learning multi-stage tasks via pixel-level translation of human videos. [arXiv preprint arXiv:1912.04443](#), 2019. 2
- [33] Jiaming Song, Chenlin Meng, and Stefano Ermon. Denoising diffusion implicit models, 2022. 6
- [34] Simon Stepputtis, Joseph Campbell, Mariano Phielipp, Stefan Lee, Chitta Baral, and Heni Ben Amor. Language-conditioned imitation learning for robot manipulation tasks, 2020. 5
- [35] Richard S Sutton, Doina Precup, and Satinder Singh. Between mdps and semi-mdps: A framework for temporal abstraction in reinforcement learning. *Artificial intelligence*, 112(1-2):181–211, 1999. 1
- [36] Homer Walke, Kevin Black, Abraham Lee, Moo Jin Kim, Max Du, Chongyi Zheng, Tony Zhao, Philippe Hansen-Estruch, Quan Vuong, Andre He, Vivek Myers, Kuan Fang, Chelsea Finn, and Sergey Levine. Bridgedata v2: A dataset for robot learning at scale, 2024. 5, 6
- [37] Haoyu Xiong, Quanzhou Li, Yun-Chun Chen, Homanga Bharadhwaj, Samarth Sinha, and Animesh Garg. Learning by watching: Physical imitation of manipulation skills from human videos. In *2021 IEEE/RSJ International Conference on Intelligent Robots and Systems (IROS)*, pages 7827–7834. IEEE, 2021. 2
- [38] Yinfei Yang, Daniel Cer, Amin Ahmad, Mandy Guo, Jax Law, Noah Constant, Gustavo Hernández Ábrego, Steve Yuan, Chris Tar, Yun-Hsuan Sung, Brian Strope, and Ray Kurzweil. Multilingual universal sentence encoder for semantic retrieval. *CoRR*, abs/1907.04307, 2019. 5
- [39] Edwin Zhang, Yujie Lu, William Wang, and Amy Zhang. Lad: Language control diffusion: efficiently scaling through space, time, and tasks. [arXiv preprint arXiv:2210.15629](#), 2023. 2, 5, 7
- [40] Edwin Zhang, Yujie Lu, William Wang, and Amy Zhang. Language control diffusion: Efficiently scaling through space, time, and tasks. [arXiv](#), 2023. 2
- [41] Lvmin Zhang and Maneesh Agrawala. Adding conditional control to text-to-image diffusion models. [arXiv preprint arXiv:2302.05543](#), 2023. 2, 4
- [42] Yifeng Zhu, Peter Stone, and Yuke Zhu. Bottom-up skill discovery from unsegmented demonstrations for long-horizon robot manipulation. *IEEE Robotics and Automation Letters*, 7(2):4126–4133, 2022. 1

A. Examples of subgoal generation with different sizes of training set

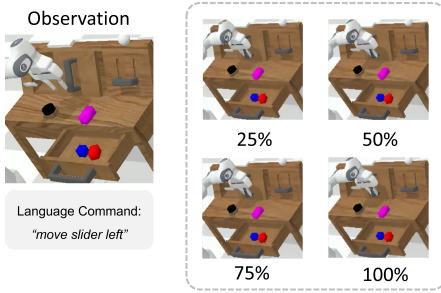


Figure 7. The generated subgoals using models trained with different amounts of data. The generated subgoals are nearly identical across varying dataset sizes.

B. Example of subgoal generation on unseen tasks and environment

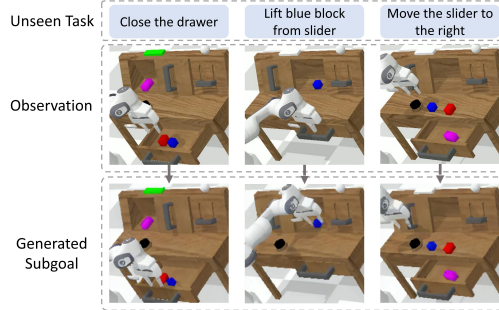


Figure 8. Example rollouts demonstrate how the generated subgoals guide the robot to perform unseen tasks.

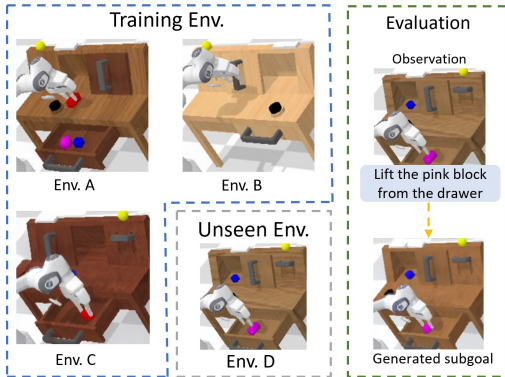


Figure 9. TaKSIE is trained using environment A, B, and C, and then tested on an unseen environment D. The example on the right demonstrates that even in an unseen environment, the model is capable of generating realistic subgoals.

C. Example of failures cases

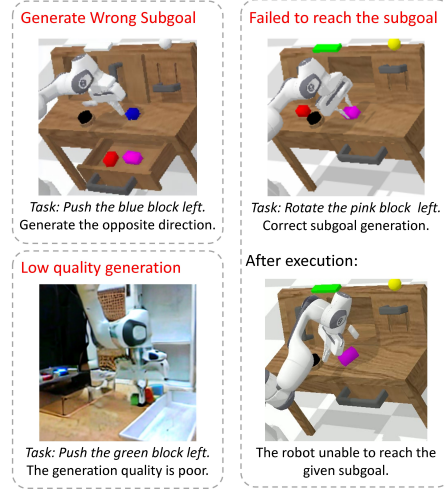


Figure 10. Three common failure cases: (1) incorrect subgoals, (2) low-quality images, and (3) failure to reach valid subgoals.

D. Comparison of different image-conditioned diffusion model

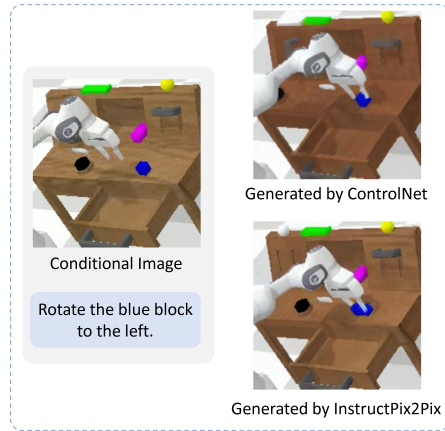


Figure 11. Comparison of subgoal generation using different image-conditioned diffusion models.

In our tests, both InstructPix2Pix and ControlNet demonstrate similar performance in seen environments. However, for unseen environments, we observe that InstructPix2Pix tends to perform better at following the conditioned environment. Fig. 11 provides an example comparison: both ControlNet and InstructPix2Pix are trained on environments A, B, and C from CALVIN and tested on the unseen environment D. InstructPix2Pix generates subgoals that appear more aligned with the conditions of environment D, while ControlNet is more aligned with environ-

δ_1	δ_2	Avg. Num. of Selected Subgoals	Avg. SR (%)
0.02	-0.02	1.02	85.51
0.01	-0.01	1.07	83.99
0.002	-0.002	1.61	76.17
0.001	-0.001	2.03	86.57

Table 6. Number of selected subgoals and success rate (SR) of different slope values for δ_1 and δ_2 . The smaller δ_1 and larger δ_2 lead to select more subgoals.

ment C, showing less effective generalization to unseen environments. This observation suggests that InstructPix2Pix may have an advantage in generalizing to new scenarios.

E. Ablation: Slope Values

The slope parameters can affect the selection of subgoals. We experiment with different δ_1 and δ_2 values in all tasks of the CALVIN validation set. Tab. 6 shows that smaller δ_1 and larger δ_2 lead to capture more subgoals. Overall, the number of our selected subgoals is less than SuSIE which selects 3 subgoals on average. Compared to SuSIE’s success rate (79.73% in Tab. 4), most of our slope values can perform better, indicating that our selected subgoals can still guide the policy. However, our experiments show no direct relationship between the number of selected subgoals and the success rate as the performance depends on the informativeness of the selected subgoals rather than the number of subgoals.